JFE TECHNICAL REPORT
No. 27 (Mar. 2022)

Ferritic Stainless Steels JFE445NT and JFE443MT with Excellent Weld Corrosion Resistance

ISHII Tomohiro[*1] SUGIHARA Reiko[*2] KOBORI Katsuhiro[*3]

Abstract:

Stainless steel is often used in severe corrosive environment due to its excellent corrosion resistance, and a slight decrease in corrosion resistance caused by welding may become a problem. In this study, the effects of additive elements on sensitization of the weld zone and corrosion in the weld crevice were investigated. It was found that increasing the contents of Nb+1.28 Ti in proportion to the increase of C+N contained in the steel was effective for sensitization control. This study also revealed that the effect of Mo on the corrosion resistance of the weld crevice is more remarkable than that of Cr, and the corrosion depth can be decreased by addition of 0.5 Mo. Based on this knowledge, the ferritic stainless steels JFE445NT and JFE443MT with excellent weld corrosion resistance were developed. These new steels are general-purpose ferritic stainless steels that can be used in a wide range of applications.

1. Introduction

Stainless steel has excellent corrosion resistance and is often used in applications in severe corrosion environments. However, it is known that the corrosion resistance necessary for the environment is reduced by welding, and this may result in severe corrosion damage[1]. There are two main causes of the reduction of the corrosion resistance of ferritic stainless steel by welding. One is a phenomenon in which the Cr concentration in the base metal decreases locally due to precipitation of chromium carbonitride by welding, and corrosion resistance decreases[2]. This phenomenon is generally called sensitization. The other is a phenomenon in which oxidization of the stainless steel surface by welding decreases the Cr concentration at the surface, leading to a decrease in corrosion resistance[3].

One severe corrosion environment in which the decrease in the corrosion resistance of the weld zone requires attention is the water tank of electric water heaters. SUS316 (18Cr-10Ni-2Mo) was used in this application in the past, but SUS444 (19Cr-2Mo) was applied from an early stage due to the problem of stress corrosion cracking. Later, a changeover to ferritic stainless steel equivalent to SUS445J1 with a reduced Mo content was promoted from the viewpoint of material cost reduction by resource conservation. JFE Steel also developed the low Mo stainless steel JFE445M (22.5Cr-1Mo-0.3Nb) for electric water heaters, which provides enhanced corrosion resistance of the temper color zone during welding[4], and has continued to supply this product to electric water heater manufacturers.

In this study, the effect of additive elements on sensitization of the weld metal and the effect of Cr and Mo on corrosion in weld crevices were investigated in detail, and the ferritic stainless steels JFE445NT (22.5Cr-1Mo-Ti, Nb) and JFE443MT (21Cr-0.5Mo-Ti, Nb) were developed. Although these new stainless steels were originally developed for the electric water heater, they are applicable to a wide range of applications because of their highly versatile component design. This paper reports the knowledge obtained in the development of these new stainless steels.

† Originally published in *JFE GIHO* No. 48 (Aug. 2021), p. 19−25

*1 Senior Researcher Manager,
Stainless Steel & Iron Powder Research Dept.,
Steel Res. Lab.,
JFE Steel

*2 Executive Assistant,
General Manager,
Stainless Steel & Iron Powder Research Dept.,
Steel Res. Lab.,
JFE Steel

*3 Staff Deputy General Manager,
Stainless Steel Sec. Products Design & Quality Control Dept.,
East Japan Works (Chiba),
JFE Steel

2. Experimental Method

2.1 Sample Materials

The chemical composition of the samples used in the experiment is shown in **Table 1**. Small steel ingots of this chemical composition were prepared in the laboratory by vacuum melting, and cold-rolled sheets with a thickness of 0.8 mm were prepared through hot rolling at a heating temperature of 1 200˚C, hot-rolled sheet annealing at 1 050˚C for 60 s, cold rolling, and cold-rolled sheet annealing at 960˚C for 60 s, and were then used in the experiment.

2.2 Welding Conditions

2.2.1 Bead on plate welding

60×200 mm specimens were taken from cold-rolled sheets and degreased with acetone, and weld beads were formed by TIG bead-on-plate welding in the longitudinal direction in the center of the specimen width. The welding speed was 60 cm/min, and the welding current was 90 A. The shielding gas used was 100 to 98% Ar with 0 to 2% nitrogen, and the shielding gas flow rate was 15 L/min.

2.2.2 Butt welding

Sample materials with a size of 30×200 mm were taken from cold-rolled sheets and SUS316L. After acetone degreasing, butt-welded 60×200 mm specimens were prepared by TIG welding by butting SUS316L against the sample materials. The groove was an I-groove, the welding speed was 60 cm/min, and the welding current was 90 A. The shielding gas was 98% Ar-2% N_2, and the gas flow rate was 15 L/min.

2.2.3 Lap fillet welding

Specimens with sizes of 60×200 mm and 20×200 mm were taken from cold-rolled sheets. The 20×200 mm specimen was superimposed on the larger specimen so that the weld bead was at the center of width of the 60×200 mm specimen, and lap fillet welding was carried out by TIG. The welding speed was 60 cm/min, the welding current was 90 to 110 A, the shielding gas was 100% Ar, and the gas flow rate was 15 L/min.

Table 1 Chemical composition of samples (mass%)

C	Cr	Mo	Ti	Nb	N
0.003 ～0.011	18.0 ～23.1	0.0 ～2.0	0.00 ～0.44	0.00 ～0.51	0.006 ～0.018

2.3 Electrochemical Measurement

2.3.1 Electrochemical potentiokinetic reactivation ratio measurement

20×20 mm specimens were taken from the bead-on-plate-welded specimen with the weld bead centered. The surface of the test piece on the welding torch side was polished until the weld bead became flat. The surface finish was #600 polished using emery polishing paper. A stainless steel wire for conduction was spot welded to the specimen, which was then coated with silicone sealant except for a 4×10 mm evaluation area on the weld bead.

Next, in a solution of 0.01 mol/L potassium thiocyanate in 0.5 mol/L sulfuric acid at 30˚C, the potential was held at the open circuit potential for 5 min, after which the potential was inserted to the noble side at an insertion rate of 100 mV/min to 150 mV (vs. SCE), and then immediately inserted to the base side. The percentage of the ratio of the active dissolution currents in the outward and homeward directions was used as the reactivation ratio.

2.3.2 Pitting potential and protection potential measurement

From the specimen prepared by lap fillet welding, 30×20 mm specimens were taken in such a way that half of the specimen had a weld crevice of 15×20 mm. A stainless wire for conduction was spot welded to the end without the weld crevice, and a 5 mm area at the edge including the stainless wire was covered with silicone sealant. Specimens of 30×20 mm were also taken from the samples without welding, a stainless steel wire for conduction was spot welded, and 5 mm at the edge was covered with silicone sealant.

Using the specimen thus prepared, the specimen was first held at a natural immersion potential in a 3.5% NaCl solution at 30˚C for 10 min, after which a potential was applied to the noble side at 100 mV/min until the current reached 1 mA, and then immediately to the base side at 100 mV/min after the current reached 1 mA. A potential of 100 μA on the outward path was defined as the pitting potential, and a potential of 100 μA on the homeward path was defined as the protection potential.

2.3.3 Anodic polarization curve measurement

Specimens of 20×20 mm were taken from the sample without welding, and a #600 polishing finish was made with emery polishing paper. A stainless steel wire for conduction was spot welded, and after acetone degreasing, the specimen was covered with silicone sealant except for a 10 × 10 mm evaluation area. After

holding at −700 mV (vs SSE) for 10 min, the polarization curves were measured at 50 mV/min from the open circuit potential to 1.2 V in a 1 mol/L NaCl solution adjusted to pH 0.5 with sulfuric acid.

2.4 Cyclic Corrosion Tests

2.4.1 Cyclic corrosion test of weld bead

Specimens with a size of 60×80 mm were taken from bead-on-plate-welded and butt-welded specimens so that the weld bead was in the width center of the longitudinal direction. The weld beads were polished on the surface on the welding torch side until the bead became flat, and a #600 polishing finish was made using emery polishing paper. Acetone degreasing was carried out, the edge and back face were covered with seal tape, and the specimens were subjected to a cyclic corrosion test. As the cycle conditions, one cycle comprised salt spray (5% NaCl, 35˚C) 2 h, dry (60˚C, R.H. : 30%) 4 h and wet (50˚C, R.H.: not less than 95%) 2 h, and the test was carried out for 15 cycles.

2.4.2 Cyclic corrosion test of weld crevice

Specimens of 60×80 mm were taken from the lap fillet welded specimen so that the weld bead was in the center of width, and after acetone degreasing, the specimens were subjected to a cyclic corrosion test under the same conditions as in 2.4.1 for a total of 30 test cycles. After the cyclic corrosion test, the weld crevice of the specimen was disassembled, and the rust in the crevice was removed using 10% nitric acid. The corrosion depth inside the crevice was measured by the depth of focus method using an optical microscope, and the average corrosion depth was obtained from the maximum depth of 10 points.

2.5 Weld Bead Component Analysis

The weld bead was cut from the welded sample, and the HAZ and surface scale were removed with a grinder. The obtained weld bead was rolled and crushed, and the chemical components were analyzed by wet analysis.

3. Experimental Results and Discussion

3.1 Effect of Additive Elements on Sensitization of Weld Zone

3.1.1 Effect of welding conditions on sensitization of weld zone

JFE445M, which is a conventional stainless steel for electric water heaters, is not sensitized by butt welding with SUS316L, and its corrosion resistance is not reduced. Therefore, the effect of nitrogen on sensitization behavior was examined by mixing nitrogen in the shielding gas used in welding in order to evaluate the welding conditions under which sensitization occurs.

Figure 1 shows the effect of the amount of nitrogen in the shielding gas on the composition of the weld metal in bead-on-plate welding. As the nitrogen content of the shielding gas increased from 0% to 2.0%, the nitrogen content of the weld metal increased from 0.008% to 0.039% and Nb/(C+N) decreased from 19.9 to 6.3.

Figure 2 shows the effect of the nitrogen content of the shielding gas on the composition of the weld metal in butt welding of JFE445M and SUS316L. The penetration ratio of SUS316L was 39% to 50%, and C and N contents in the weld metal increased and Nb/(C+N) decreased compared with bead-on-plate welding.

After the weld beads were flattened by polishing, cyclic corrosion tests of these welded specimens were carried out for 15 cycles. The occurrence of corrosion from the weld bead is shown in **Table 2**.

In bead-on-plate welding, sensitization of the weld

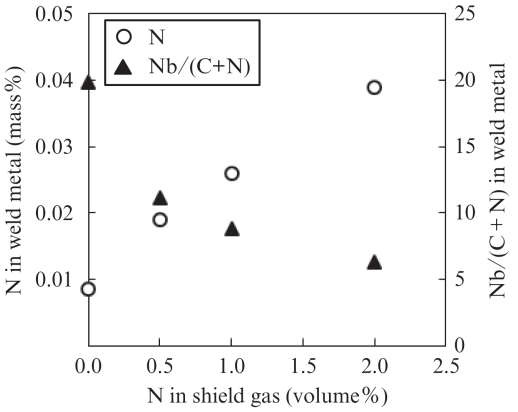

Fig. 1 Effect of N content of shield gas on composition of weld metal in bead-on-plate welding of JFE445M

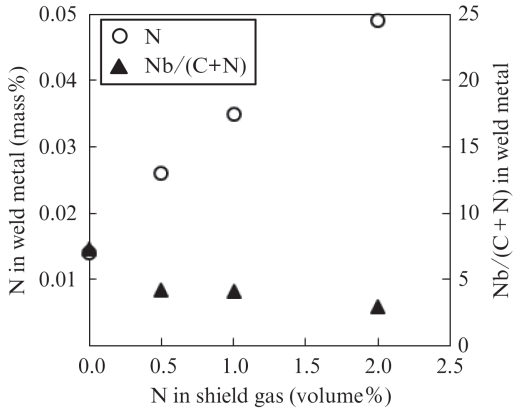

Fig. 2 Effect of N content of shield gas on composition of weld metal in butt welding of JFE445M and SUS316L

Table 2 Existence of corrosion by cyclic corrosion test of weld bead welded with nitrogen mixed shield gas

	N in shield gas			
	0%	0.5%	1.0%	2.0%
Bead on plate	○	○	○	×
Butt welding	○	○	×	×

CCT 15cycles, ○: No corrosion, ×: Corrosion

metal occurred when the nitrogen content of the shielding gas was 2.0%, and in this case, corrosion occurred. Since Nb/(C+N) of the weld metal with a 1.0% nitrogen content is 8.8 and Nb/(C+N) of the 2.0% nitrogen weld metal is 6.3, it is suggested that sensitization may occur at Nb/(C+N) of 8 or less in bead-on-plate welding.

On the other hand, in butt welding with SUS316L, corrosion occurred at 1.0% and 2.0% nitrogen contents of the shielding gas. The Nb/(C+N) of the weld metal was 4.2 with 0.5% nitrogen in the shielding gas, where no corrosion occurred, and 4.1 at 1.0% nitrogen, where corrosion occurred. The sensitization threshold was lower than that for bead-on-plate welding because the weld bead consisted of the two phases of austenite and ferrite, and carbon and nitrogen were dissolved in the austenite phase as a result of welding with SUS316L.

As described above, in both bead-on-plate welding and butt welding, sensitization occurred when 2.0% nitrogen was mixed in the shielding gas. Therefore, in subsequent sensitization tests of the weld bead, sensitization was evaluated by using Ar gas containing 2.0% nitrogen as the shielding gas.

3.1.2 Effect of stabilizing elements on sensitization of weld zone

The stabilizing elements Ti and Nb are known to suppress the sensitization of welds. In order to evaluate the effect quantitatively, the electrochemical potentiokinetic reactivation ratio was measured using specimens which were bead-on-plate welded to specimens with various Ti and Nb contents.

An example of the measured polarization curve is shown in **Fig. 3**. Since the stainless steel used in this experiment has high corrosion resistance, the active dissolution peak (B) appeared slightly after the cathodic current was measured on the homeward path. The ratio B/A×100 of the maximum value of active dissolution (B) measured on the homeward path to the maximum value of active dissolution (A) measured on the outward path was used as the reactivation ratio.

Figure 4 shows the effect of the stabilizing elements on the electrochemical potentiokinetic reactivation ratio of weld beads welded with shielding gas containing 2.0% nitrogen. A good correlation was observed

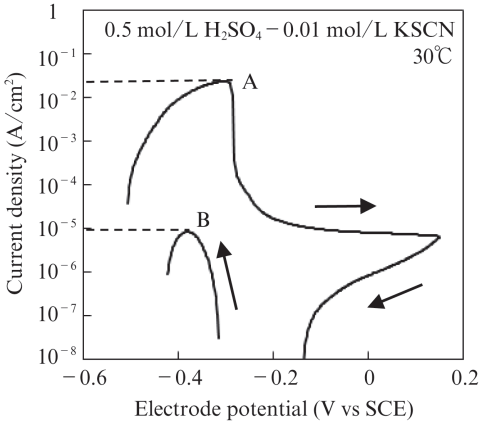

Fig. 3 Polarization curve of electrochemical potentiokinetic reactivation measurement

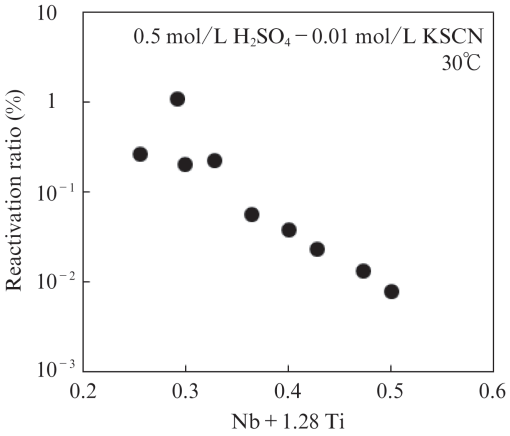

Fig. 4 Effect of stabilizing element on electrochemical potentiokinetic reactivation of weld bead

between the logarithm of the reactivation ratio and Nb+1.28 Ti. Since the reactivation ratio of the weld bead was proportional to Nb+1.28 Ti, it is suggested that the sensitization behavior of the weld zone can be controlled by adjusting the amount of Nb and Ti added in line with this ratio.

3.1.3 Effect of C and N on sensitization of weld zone

In order to consider the appropriate amounts of Ti and Nb to be added, specimens with various C, N, Ti and Nb contents were butt welded with SUS316L, and the sensitization of the weld zone was evaluated by a 15 cycle corrosion test. **Figure 5** shows the results of the cyclic corrosion test. As C+N in the steel increases, a larger amount of stabilizing elements is required to suppress sensitization of the weld zone. The solid line in this figure represents the formula Nb+1.28 Ti = 6.2 (C+N)+0.37. The region where the stabilizing elements are more abundant than this line shows good sensitiza-

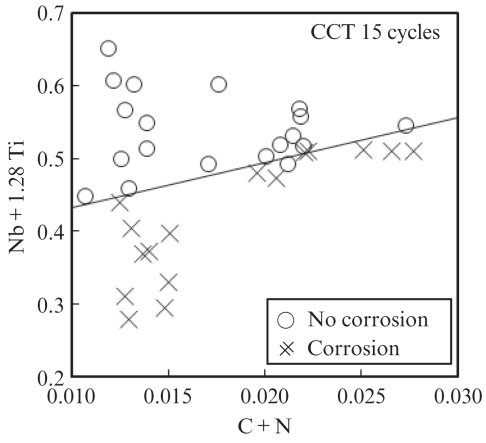

Fig. 5 Effect of C, N, Nb and Ti on sensitization of butt welding with SUS316L

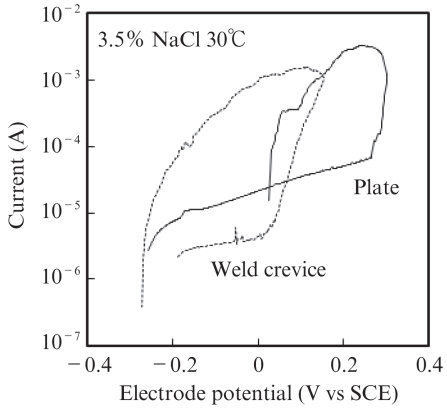

Fig. 6 Polarization curve of protection potential of plate and weld crevice specimen

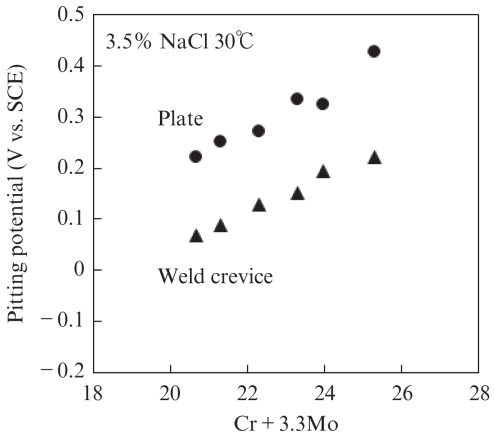

Fig. 7 Effect of Cr and Mo on pitting potential of plate and weld crevice specimen

tion behavior, without corrosion from the weld zone. Therefore, it is considered that stainless steel with good sensitization resistance can be obtained by controlling the contents of Nb+1.28 Ti to an appropriate addition quantity in proportion to C+N in the steel.

Based on this result, the developed steels JFE445NT and JFE443MT are designed to have chemical compositions in which sensitization of the weld zone is difficult by appropriate adjustment of the amounts of added C, N, Nb and Ti.

3.2 Effect of Cr and Mo on Weld Crevice Corrosion

3.2.1 Effect of Cr and Mo on initiation and repassivation of corrosion in weld crevice

Corrosion easily occurs in the weld crevice as a result of welding oxidation, and often becomes a problem in actual use. Therefore, in order to examine the initiation of corrosion and repassivation in the weld crevice, the pitting potential and protection potential were measured by using a flat plate specimen and a specimen with a weld crevice prepared from test materials with various Cr and Mo contents.

An example of the measured polarization curve is shown in **Fig. 6**. The pitting corrosion potential and protection potential were measured for both the flat plate and the weld crevice. Compared with the flat plate specimen, the weld crevice specimen showed a slower current rise after pitting corrosion and a slower current drop during potential insertion to the base side. This is because the movement of the solute is suppressed by the crevice shape.

The pitting potentials of the plate specimen and the weld crevice specimen are shown in **Fig. 7**. The pitting potential was proportional to the pitting index Cr+3.3Mo for both the flat plate specimen and the weld crevice specimen. The proportional coefficient of the pitting potential against Cr+3.3Mo was 38 mV, and the average difference in the pitting potential between the weld crevice specimen and the flat plate specimen was 163 mV.

The measurement results of the protection potential are shown in **Fig. 8**. As in the case of the pitting potential, the protection potential was also proportional to Cr+3.3Mo in both the plate specimen and the weld crevice specimen, and the proportional coefficient was 40 mV. The average difference between the flat plate specimen and the weld crevice specimen was 126 mV.

The difference in the protection potential between the flat plate specimen and the weld crevice specimen is smaller than the difference in the pitting potential. Therefore, the potential increase by eliminating the weld crevice is smaller in the protection potential than in the pitting potential. Dividing the difference in the protection potential of 126 mV by the propotional coefficient of 40 mV relative to Cr+3.3Mo yields 3.2. That is to say, even if the content of Cr and Mo is

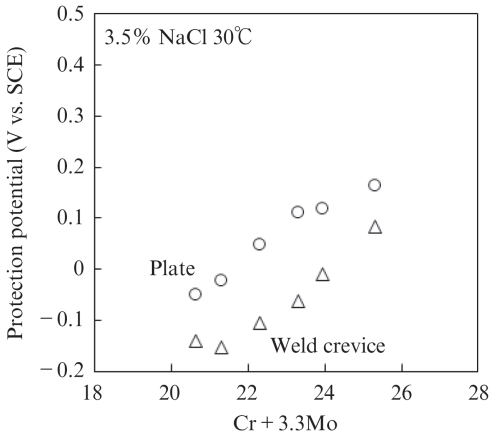

Fig. 8 Effect of Cr and Mo on protection potential of plate and weld crevice specimen

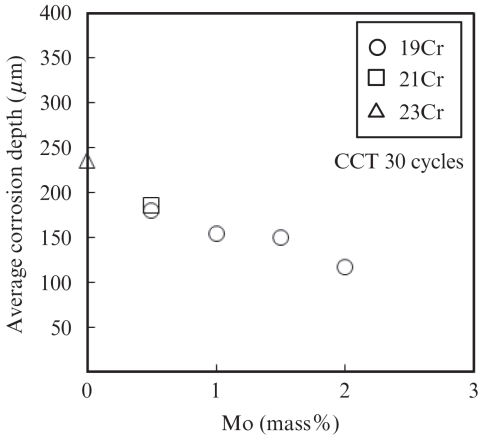

Fig. 10 Effect of Mo on corrosion depth of crevice specimen

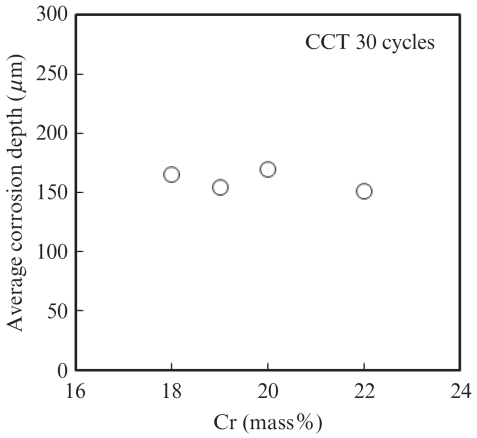

Fig. 9 Effect of Cr on corrosion depth of crevice specimen

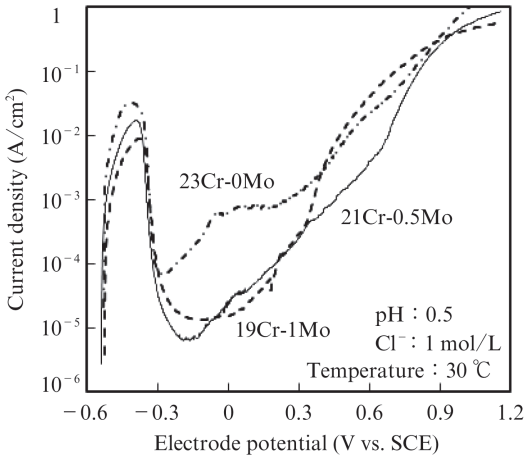

Fig. 11 Effect of Cr and Mo on polarization curve in low pH and high Cl^- environment

reduced by 3.2 in terms of the pitting index Cr+3.3Mo, the protection potential becomes equivalent by changing the weld crevice to a flat plate, indicating that equivalent corrosion resistance is obtained in the initiation of corrosion and repassivation.

3.2.2 Effect of Cr and Mo on corrosion propagation in weld crevice

In order to evaluate the propagation behavior of corrosion in the weld crevice, cyclic corrosion tests were carried out using lap fillet welded specimens.

Figure 9 shows the effect of Cr on the corrosion depth of crevice corrosion. The corrosion depth of 18Cr was 165 μm, while that of 22Cr was 151 μm.

Figure 10 shows the effect of Mo on the corrosion depth of crevice corrosion. Although Cr ranged from 19% to 23%, the corrosion depth decreased on the same line when the Mo content was increased, showing that the effect of Mo was dominant for the change in the corrosion depth. The corrosion depth of 0 Mo was 236 μm, while that of 0.5 Mo was 180 μm.

Figure 11 shows the effect of Cr, Mo on the polarization curve in a low-pH, high-Cl environment. In 23Cr-0Mo, sufficient passivation does not occur, and the passive current is high. However, in the 21Cr-0.5Mo, the passive current decreased, resulting in the appearance of a passivation region. The crevice corrosion environment was low pH and high Cl^-, and it is considered that this change in the polarization curve by Mo addition affected the corrosion propagation behavior and decreased the corrosion depth.

4. Corrosion Resistance of Weld Zone of Developed Steels

Based on the above results, the ferritic stainless steels JFE445NT (22.5Cr-1Mo-Ti, Nb) and JFE443MT (21Cr-0.5Mo-Ti, Nb) with excellent corrosion resistance of welds were developed.

As shown in **Fig. 12**, the developed JFE445NT and JFE443MT display good corrosion resistance in butt

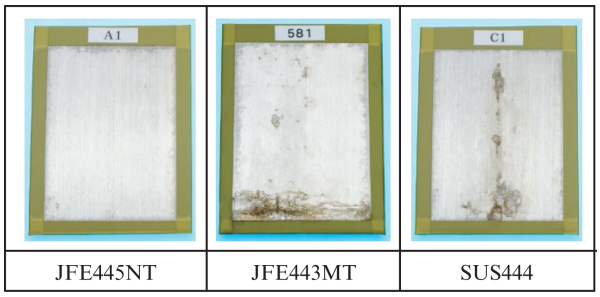

Fig. 12 Comparison of sensitization behavior of butt weld between SUS316L and JFE445NT, JFE443MT, SUS444. CCT 15 cycles

welding with low C austenitic stainless steels such as SUS316L. With general austenitic stainless steels such as SUS304, a weld bead with good corrosion resistance can be obtained by using YS316L as the welding wire.

5. Conclusion

The ferritic stainless steels JFE445NT and JFE443MT, which are superior in corrosion resistance of welds, were developed based on a detailed study of the sensitization behavior of various types of welds and the effect of additive elements on the corrosion behavior of the weld crevice. The following knowledge was obtained in the development process of these new steels.

(1) The logarithm of the reactivation ratio of the weld zone was proportional to Nb+1.28 Ti, and the decrease in corrosion resistance caused by sensitization of the weld zone decreased with increasing Nb+1.28 Ti.

(2) As the C and N contents in the steel increased, the addition of Nb and Ti required to suppress sensitization of the weld zone also increased. Sensitization of welds does not occur when the additive elements satisfy the formula Nb+1.28 Ti$\geqq$6.2 (C+N)+0.37.

(3) The pitting potential and protection potential were proportional to the pitting index Cr+3.3Mo in both the weld crevice and flat plate specimens. In the flat plate specimen, the pitting potential and protection potential can be made equal or higher than those of the weld crevice specimen even if the pitting number is lowered by 3.2.

(4) Although the effect of Cr on the depth of crevice corrosion was slight, addition of 0.5Mo decreased the depth of crevice corrosion.

(5) The developed steels, JFE445NT and JFE443MT, show good corrosion resistance in butt welding with SUS316L, and are general-purpose stainless steels applicable to a wide range of applications.

References

1) Onishi, M. Corrosion resistance of steel welds. Corrosion Engineering. 1964, vol. 13, p. 289–295.
2) Matsushima, I. Weld corrosion (III). Journal of Welding Society. 1992, vol. 61, p. 144–152.
3) Kono, T.; Ishii, T.; Kajiyama, H.; Kimura, M.; Fushimi, K. Local Electrochemical Behavior of Welding Heat Tint Parts of Stainless Steel. Zairyo-to-Kankyo. 2015, vol. 64, p. 552–557.
4) Fukuda, K.; Ishikawa, S.; Kasashige, T. Mo-saving Stainless Steel JFE 445M for Hot Water Tanks. JFE Technical Report. 2008, no. 12, p. 57–64.